Received: 24 September 2020 | Revised: 10 December 2020 | Accepted: 5 January 2021

DOI: 10.1002/bdr2.1870

REVIEW ARTICLE

Birth Defects Research | THE TERATOLOGY SOCIETY | WILEY

Single-cell profiling for advancing birth defects research and prevention

Thomas B. Knudsen[1] | **Malte Spielmann**[2,3] | **Sean G. Megason**[4] | **Elaine M. Faustman**[5]

[1]Center for Computational Toxicology and Exposure, U.S. Environmental Protection Agency, Research Triangle Park, North Carolina

[2]Human Molecular Genomics, Max Planck Institute for Molecular Genetics, Berlin, Germany

[3]Institute of Human Genetics, University of Lübeck, Lübeck, Germany

[4]Department of Systems Biology, Harvard Medical School, Boston, Massachusetts

[5]Department of Environmental & Occupational Health Sciences, University of Washington, School of Public Health, Seattle, Washington

Correspondence
Thomas B. Knudsen, Center for Computational Toxicology and Exposure, U.S. Environmental Protection Agency, Research Triangle Park, NC.
Email: knudsen.thomas@epa.gov

Abstract

Cellular analysis of developmental processes and toxicities has traditionally entailed bulk methods (e.g., transcriptomics) that lack single cell resolution or tissue localization methods (e.g., immunostaining) that allow only a few genes to be monitored in each experiment. Recent technological advances have enabled interrogation of genomic function at the single-cell level, providing new opportunities to unravel developmental pathways and processes with unprecedented resolution. Here, we review emerging technologies of single-cell RNA-sequencing (scRNA-seq) to globally characterize the gene expression sets of different cell types and how different cell types emerge from earlier cell states in development. Cell atlases of experimental embryology and human embryogenesis at single-cell resolution will provide an encyclopedia of genes that define key stages from gastrulation to organogenesis. This technology, combined with computational models to discover key organizational principles, was recognized by Science magazine as the "Breakthrough of the year" for 2018 due to transformative potential on the way we study how human cells mature over a lifetime, how tissues regenerate, and how cells change in diseases (e.g., patient-derived organoids to screen disease-specific targets and design precision therapy). Profiling transcriptomes at the single-cell level can fulfill the need for greater detail in the molecular progression of all cell lineages, from pluripotency to adulthood and how cell–cell signaling pathways control progression at every step. Translational opportunities emerge for elucidating pathogenesis of genetic birth defects with cellular precision and improvements for predictive toxicology of chemical teratogenesis.

KEYWORDS

birth defects, developmental toxicity, single cell profiling, single cell RNA-seq

1 | INTRODUCTION

A major goal of developmental biology is to understand the detailed molecular progression of all embryonic cell lineages, from pluripotency to adulthood, and how cell–cell signaling pathways control lineage choices at every

The views expressed in this article are those of the authors and do not necessarily reflect the views or policies of the U.S. Environmental Protection Agency. Mention of trade names or commercial products does not constitute endorsement or recommendation for use.

step of differentiation. Technologies for profiling regulation of the embryonic transcriptome with single-cell resolution have emerged as a key research area for this purpose, and consequently set the stage for a mechanistic understanding of developmental defects. The symposium on "Single-cell Revolution: Embryogenesis at High-Resolution" presented at the 60th Annual Meeting of the Society of Birth Defects Research and Prevention covered some of the main concepts in single-cell profiling, how the emerging technology is shaping our understanding of embryo development, and opportunities and challenges for elucidating teratological mechanisms with single cell precision (https://www.birthdefectsresearch.org/meetings/2020/).

Next-generation sequencing (e.g., RNA-seq) made possible through advances in the genomic sciences have put molecular profiling at the forefront of understanding how the embryo reacts to physiological queues imposed during developmental processes and toxicities. Bulk tissue analysis averages these effects within a cell population and thereby masks the cellular resolution needed to pinpoint the response. Spatial localization techniques such as in situ hybridization and immunohistochemistry can localize these responses but for only a few genes or proteins at a time. Single cell transcriptomics (scRNA-seq) enables a comprehensive understanding of gene expression dynamics that program or reflect individual cell states in response to genetic signals, to physiological queues in the microenvironment, and/or cellular adaptation to toxicological stress. This enables comprehensive analysis at the fundamental unit of tissue organization - the cell, where each has its own unique lineage, state dynamics, and microphysiology. Combining scRNA-seq with other single-cell modalities (e.g., *in toto* imaging, CRISPR/Cas9) and reconstructive computational biology is a powerful new approach to understand the molecular cartography of patterning systems during embryogenesis and pathogenesis (Cao et al., 2019; Chan et al., 2019; Keller, Schmidt, Wittbrodt, & Stelzer, 2008; McDole et al., 2018; McKenna & Gagnon, 2019; Megason, 2009; Pijuan-Sala et al., 2019; Sladitschek et al., 2020).

2 | SINGLE-CELL TRANSCRIPTOMICS WORKFLOW

First introduced in 2009, scRNA-seq now has over 385 approaches (as of March 2019) to predict cell fates in differentiation (Leuken & Theis, 2019; Ziegenhaein et al., 2017). A typical workflow is shown (Figure 1).

2.1 | Sample preparation

Some form of cell dissociation is needed to liberate and capture thousands of cells. A key issue is knowing how

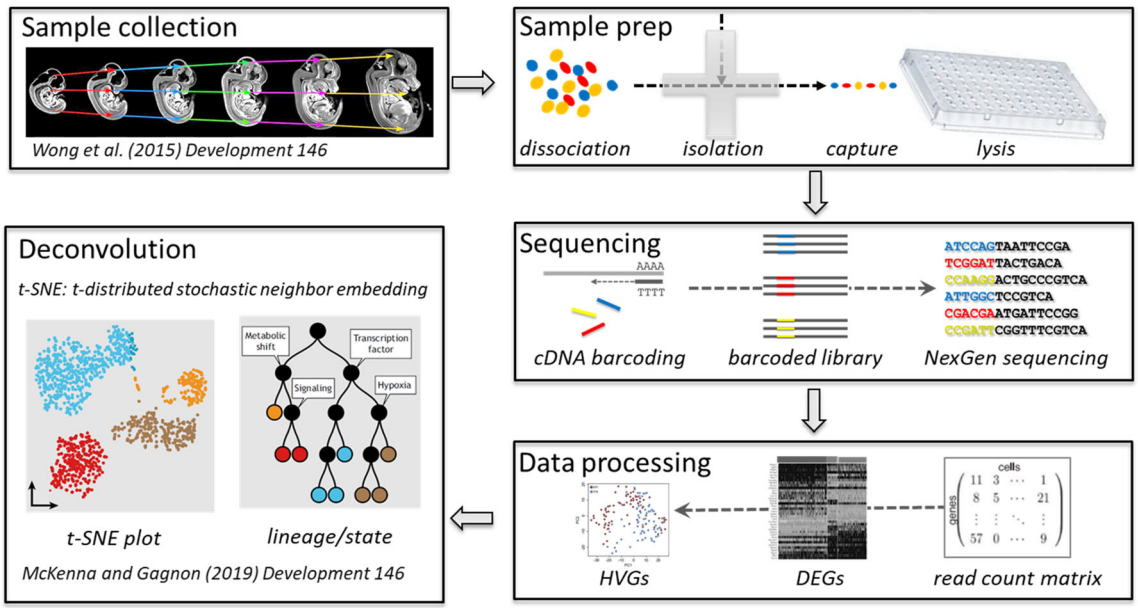

FIGURE 1 Single-cell RNA-seq reconstruction of gene expression dynamics during embryogenesis. Time-variant experimental tissue samples are prepared by various dissociation methods with microfluidics to isolate and capture individual cells for individual cDNA barcoding. After multiplex RNA-seq analysis, gene × cell matrices are normalized and processed to identify differentially expressed genes (DEGs). Those highly variable genes (HVGs) are then selected for deconvolution by analytical methods such as t-SNE (t-distributed neighbor embedding) that cluster cells by their individual HVG profile and subsequently reconstruct cell lineage and cell state relationships in pseudotime

well different cell types and their transcriptomes survive preparation protocols required to generate isolated cells from an intact tissue. Different capture methods include microwell plates (microwell-seq) (Han et al., 2018), high-throughput droplet encapsulation (Drop-Seq, inDrops) (Klein et al., 2015), or single cell combinatorial indexing (sci-seq) (Cao et al., 2017). Micro-drop methods use microfluidics to register a sample into thousands of tiny droplets that contain single cells. In practice, this is typically a Poisson distribution- many droplets have 0, some 1, and a few 2 cells. Individual cells are lysed and mRNA are reverse transcribed for multiplex sequencing.

2.2 | Sequencing

Complementary DNA (cDNA) libraries are barcoded with various labels that allow assignment to the original cell. This allows pooling of individual cell transcriptomes after reverse transcription for multiplex sequencing. The barcodes identify individual mRNAs transcribed from the same genomic sequence. The barcoding may also include labeling with unique molecular identifiers that serve to distinguish sequencing reads off the same mRNA transcript from separate mRNAs transcribed off the same gene. Protocols are tuned to optimize desired tradeoffs in throughput, read length, sequencing depth, and cell coverage (Leuken & Theis, 2019).

2.3 | Data processing

A gene x cell read count matrix is constructed by aligning reads to a reference genome or transcriptome. For quality control, several metrics are analyzed including the number of counts per barcode (count depth), number of genes per barcode (thresholds), and the fraction of counts from mitochondrial genes per barcode (a sign of broken plasma membrane). Different approaches can be used to filter out technical artifacts (e.g., dying cells, doublets), batch effects, PCR errors, and over-sequencing that can generate artificial cell clusters. This is a major area for current development of bioinformatics, especially for studies where the cost associated with sequencing depth might be reduced by focusing on specific targets (https://www.biorxiv.org/content/10.1101/551762v2). Expression levels of different genes are typically normalized so highly expressed genes do not overwhelm the signal of low expressed genes. The normalized gene x cell count matrix is the starting point for dimensionality reduction (Leuken & Theis, 2019). Differentially expressed genes (DEGs) are further identified to focus on highly variable genes (HVGs) (Klein et al., 2015). In this way, the biological manifold on which cellular expression trajectories lie can be sufficiently described by HVGs. An important tradeoff is to distinguish HVGs from sequencing artifacts.

2.4 | Deconvolution

Two common visualization techniques to cluster cells are t-distributed stochastic neighbor embedding (t-SNE) and Uniform Manifold Approximation and Projection (UMAP). A t-SNE plot, for example, maps cells to individual clusters based on nearest neighbor correlation in HVG expression profiles, conceptually similar to the way BLAST finds the closest match in a sequence database. Clusters can then be annotated based on what marker genes they contain (Kiselev, Andrews, & Hemberg, 2019). Although widely used, t-SNE is best thought of as a coarse visualization tool. It is limited by the loss of large-scale information on inter-cluster relationships, slow computation time and inability to meaningfully represent very large datasets. UMAP preserves more data structure than t-SNE and with a shorter run time (Becht et al., 2019). This provides more coverage and resolution of transitional states between main cell clusters. Cells unassigned to a main reference cluster have great potential for understanding cellular dynamics as they may reflect previously unrecognized or novel states that reflect continuous changes in the transcriptome otherwise undetected in bulk tissue analysis. Lineage and state diversification can be inferred as a developmental continuum with dynamic models of gene expression (trajectory inference) that maps cellular densities across "pseudotime." The concept of pseudotime in a single cell manifold is to reconstruct temporal relationships between cell states profiled in real time (see Saelens, Cannoodt, Todorov, & Saeys, 2019).

As continuum gene expression manifolds reduce the dimensionality of cell–cell distances to virtual pseudotime state trajectories, the question arises as to how we apply the scRNA-seq to better understand developmental processes and pathogenesis. For this purpose, a number of technical challenges must be considered beyond the usual quality-control considerations for a conventional microarray study: assessing how well the individual cell transcriptomes survive tissue dissociation protocols to generate isolated cells from a composite system; retaining individual cell provenance while deep-sequencing thousands of cells in parallel; distinguishing highly variable genes (HVGs) from technical noise (e.g., PCR artifacts and over-sequencing); and computational reconstruction of the composite system from individual cell clusters for definitive lineage progression and transitional states.

3 | ANALYSIS OF SIMPLE INVERTEBRATE MODEL ORGANISMS

Comprehensive "cell atlases" built with scRNA-seq data for simple model organisms (SMOs) demonstrate unique advantages in mapping developmental trajectories during embryogeny. For example, the SMOs *Caenorhabditis elegans*, *Planaria*, and *Drosophila* are amenable to direct cell lineage analysis and demonstrate the fundamental principle of conservation of cell signaling (Cao et al., 2017; Karaiskos et al., 2017; Plass et al., 2018).

3.1 | *C. elegans*

Notable for classical developmental lineage analysis in an anatomically simple organism, the complete cell lineage history of all 959 somatic cell nuclei in the roundworm is well characterized; however, knowledge of each cell's molecular state is fragmentary. The scRNA-seq profiles of 50,000 fixed cells captured at the L2 larval stage (762 somatic cells per larva) yielded 42,035 barcoded transcriptomes at a sequencing depth of ~20,000 reads per cell, averaging 431 HVGs per cell. The t-SNE plots formed 29 distinct cell clusters ranging from 131 to 13,205 (31.4% of the population) cells (Figure 2a). At least 10 cell types could be annotated using known marker genes, and several novel states were identified (Cao et al., 2017).

3.2 | Planaria

The flatworm is an interesting SMO for its ability to regenerate body parts from a population of pluripotent stem cells in the adult that can differentiate into the full complement of cell types and tissues. A comprehensive cell atlas built from scRNA-seq data reconstructed a tree-like lineage structure indicating the relationships (Figure 2b). This sets the stage for further studies to reverse-engineer cellular reprogramming of the regenerative lineage tree (Plass et al., 2018).

3.3 | Drosophila

As one of the quintessential animal models for developmental genetics and molecular patterning, the characterization of gene expression dynamics at a single-cell level in the fruit fly provides novel insight into the genetic organizing principles that shape the body plan (Karaiskos

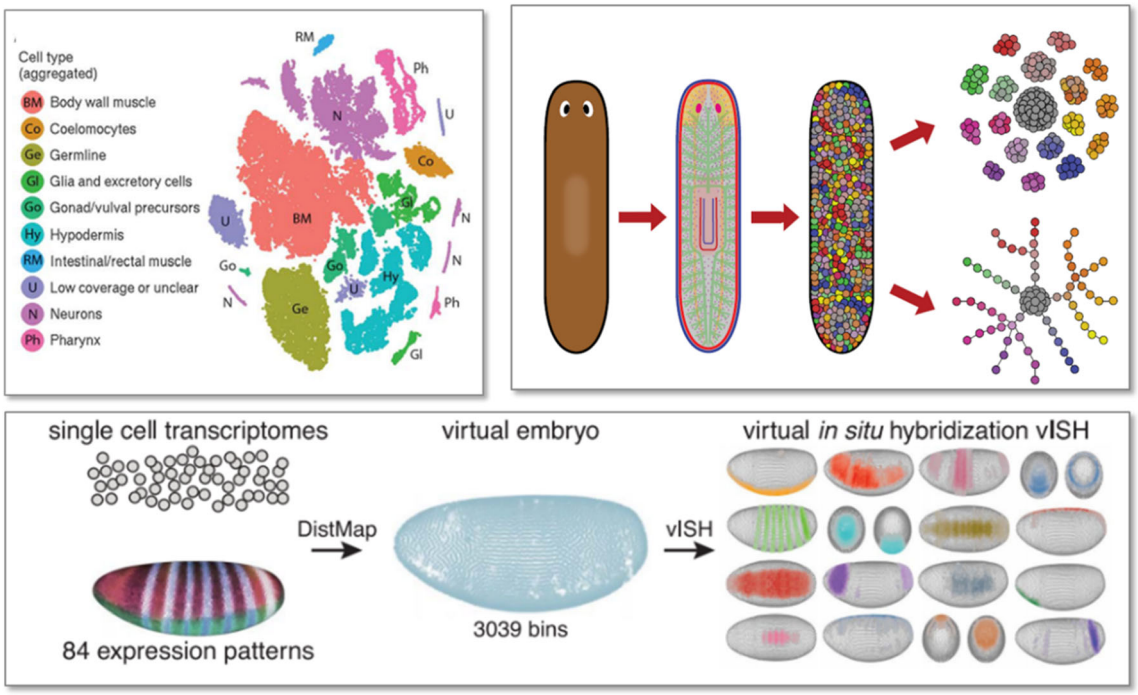

FIGURE 2 Reconstruction of spatial-temporal dynamics of gene expression defined by scRNA-seq profiling in SMO systems. (Upper left) *Caenorhabditis elegans* decomposed into 29 main clusters at the L2 larval stage (Cao et al., 2017); (upper right) decomposition of adult planaria (regenerative) into multiple cell states and computational reassembly of divergent lineages in a globally regenerative system (Plass et al., 2018); and (bottom) *Drosophila*, patterning in a digital embryo visualized during segmentation (Karaiskos et al., 2017)

et al., 2017). Drop-seq characterized >10,000 cells at a read depth of >8,000 genes per cell and tSNE plots annotated 84 cell clusters representing 87% cells in the embryo. Because many of the key transcription factors and signal-receptor gradients that drive cell cluster identity have been digitally mapped by conventional whole-mount in situ hybridization (ISH), the HVGs from t-SNE plots could be spatially reconstructed by "virtual ISH" to digitally visualize and computationally predict their developmental trajectories (Figure 2c).

4 | EXPERIMENTAL EMBRYOLOGY

Comprehensive cell atlases are built for modeling gene expression dynamics as cells acquire specified fates during morphogenesis and differentiation. Essentially, we need to understand how HVGs define, in pseudotime, the "developmental grammar" in more anatomically complex species often used for experimental embryology (e.g., *Ascidian*, *Danio*, *Xenopus*).

4.1 | Ascidian

The tunicate is an interesting SMO because it develops a notochord and dorsal hollow nerve cord, but not metameric patterning (e.g., it is an invertebrate *Chordate*), and it has a relatively simple cell lineage. Using scRNA-seq, the complete gene expression history was determined for each cell at every division up to gastrulation (2- to 64-cell stage) yielding 6.65 billion scRNA-seq reads on 1,042 cells of 58 embryos (>8 K genes per cell); furthermore, the physical position of each cell was visualized by digital light-sheet microscopy (Sladitschek et al., 2020). The combination of lineage tracing and *in toto* imaging produced an online "digital embryo" library where individual genes can be selected and visualized by vISH in a dynamic simulation as the axial body plan is established (http://digitalembryo.org). An example is shown in Figure 3a for two genes (chordin, nodal) that instruct early patterning of the notochord. Quoting the authors, "The ability to track systematically, quantitatively, and in a spatially resolved manner the genome-wide changes of gene expression of every cell at each cell division in

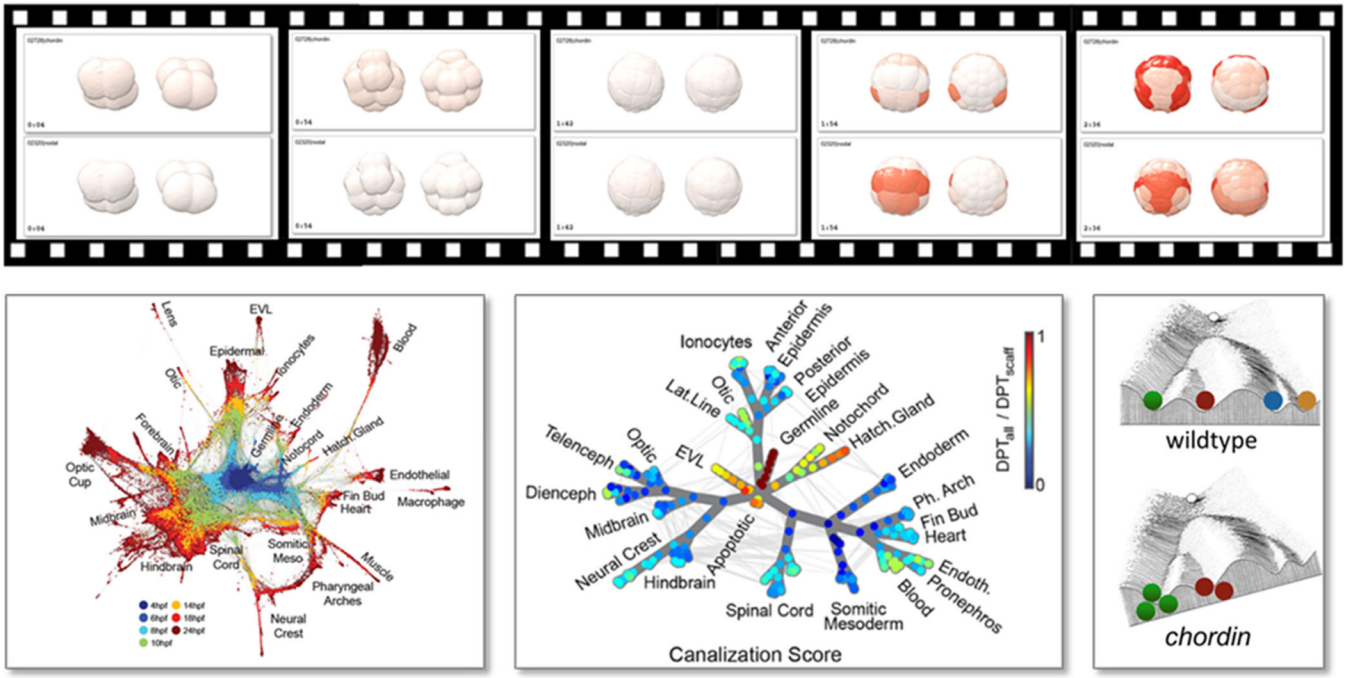

FIGURE 3 Gene expression dynamics during early development in Chordate models. (Top) *Ascidian*, showing dynamic vISH for two patterning genes selected and viewed dynamically from the vegetal pole (left image) and animal pole (right image). Simulated expression of chordin (top) and nodal (bottom) are represented in red shading between the 4- and 64-cell stage in pseudotime executed from the http://digitalembryo.org cell atlas (Sladitschek et al., 2020). (Bottom) Zebrafish developing between 4- and 24-hpf stage (Wagner et al., 2018). *Left panel*: a comprehensive map of lineage and state with cell diversification trajectories for 10^5 individual cells. *Middle panel*: canalization plot colored by trans-specification potential. *Right panel*: classical Turing-like representation of canalized cell trajectories for normal and *chordin* CRISPR/Cas9 injection; *chordin* crispants showed no new cell types but displayed a change in abundance of different cell types (from the work of Megason, Wagner, and Klein)

embryos will usher in a new era in developmental biology" (Sladitschek et al., 2020).

4.2 | Danio

Two landmark studies in zebrafish set the stage for understanding the robustness of growth and form with single-cell imaging and sequencing. In one study, Drop-seq was used to build a tree-like lineage from 38,731 cells captured from 694 embryos across 12 stages, spanning from 3.3 hr post-fertilization (hpf) (blastula, just after the onset of zygotic transcription when most cells are pluripotent) to 12 hpf (pharyngula, 6 somite stage when many cells have acquired differentiated fates) (Farrell et al., 2018). Because the pharyngula stage is phylotypic, for example, when conservation of cell signaling is most apparent in establishment of the *Vertebrate* body plan, the organizing principles are likely to be conserved as well. The lineage tree recapitulated the developmental trajectories for 25 cell clusters. Most of the annotated cell types were known from classical embryology; however, the study revealed transitional states in the progression, consistent with a continuum in the pseudogene manifold. The other landmark zebrafish study mapped the gene expression landscape using inDrops scRNA-seq on >92,000 cells across seven stages to generate a comprehensive map of cell state trajectories and cell lineage in zebrafish development through the first 24 hpf (Wagner et al., 2018). Different algorithms built for inferring expression landscapes identified critical branch points for at least 10 cell types in a continuous state manifold over time. When the scRNA-seq data was stitched into a force-directed layout colored by time, virtual fate map reconstruction revealed alternate pathways with different degrees of overlap between various trajectories. The authors assigned a "canalization score" to formally represent the robustness of trajectories and off-tree connections (Figure 3b).

Canalization (after the Turing model) refers to the tendency for development of a specific genotype to follow the same trajectory under different conditions (Hallgrímsson, Willmore, & Hall, 2002). Most developmental trajectories were weakly canalized (e.g., neural plate, somitic mesoderm) but a few were medium (notochord) or strongly canalized (germ line). Therefore, *in silico* fate-mapping along branches of the cell lineage manifold implied discordance with cell state progression (Wagner et al., 2018). To more closely evaluate how cell state evolved over time, they used "TracerSeq" lineage barcoding with *Tol2* transposon to evaluate the same cells across the manifold. The authors found that cells can be close in state but farther in lineage, displaying non-binary contiguity with broad continua of state space, complex branching patterns, and loops. The complex lineage-state architecture of gene expression dynamics reinforces the paradigm that some cells retain a multifate potential and can trans-specify from one developmental trajectory to another.

A selective advantage of canalization may be to control proper cell number during cell fate acquisition (bootstrapping) and a determinant of developmental behaviors of the system when perturbed by genetic or environmental factors (buffering). A comparison of trajectories from zebrafish (Wagner et al., 2018) to *Xenopus* (Briggs et al., 2018) revealed that orthologous genes showed variable cell state-specific expression overall (30% conserved) and that transcription factors were the most conserved. This indicates "function over sequence" where transcriptional control in the gene regulatory network and physiological genes are co-opted into pathways for specific cell signaling, metabolism, and homeostasis.

5 | MAMMALIAN EMBRYOLOGY

The vast majority of cell lineages in mammals derive from the epiblast layer of the early embryo during gastrulation and early organogenesis (embryonic days E6.5–E8.5 in mouse, Days 14–17 post-fertilization in humans). The body's fundamental blueprint is also decoded during this period through formation of the primitive streak that defines the anterior–posterior (e.g., head to tail) axis.

5.1 | Cell diversification

In mouse, gastrulation commences at the egg cylinder stage (E6.25) when cells from the posterior epiblast converge at the midline and undergo an epithelial-mesenchymal transition. The primitive streak advances anteriorly and culminates with formation of posterior regions by the headfold stage (E8.5). A t-SNE plot was developed from 116,312 cells captured for scRNA-seq at nine time points between E6.5 and E8.5, from pluripotency toward all major embryonic lineages (Pijuan-Sala et al., 2019). These authors annotated 37 main clusters based on known biomarker genes for molecular diversification of cells in the embryo proper and associated extraembryonic membranes (Figure 4a). Inferences on complex signaling were based on an innovative analysis of chimeric embryos. Embryos deficient in the transcription factor TAL1 die at E9.5 due to defects in mesodermal diversification that lead to severe anemia; however, the developmental fates of *Tal1(−/−)* cells can be tracked in chimeric embryos generated from

microinjection of labeled embryonic stem cells into the *Tal1(+/+)* blastocyst that form otherwise healthy embryos (Pijuan-Sala et al., 2019). An scRNA-seq evaluation of labeled and unlabeled cells sorted from chimeric embryos at the headfold stage (E8.5) confirmed that the mutant cells do not contribute to the hematopoietic lineage; furthermore, the reverse experiment showed that labeled *Tal1(+/+)* cells do contribute to the hematopoietic lineage when injected to host *Tal1(−/−)* embryos. Combining temporal and transcriptional information can illuminate gene function.

At E8.5, the headfold stage embryo transitions to organogenesis, expanding from hundreds-of-thousands to over ten-million cells as it forms nearly all major organ system rudiments between E9.5 and E13.5. This period was evaluated by combinatorial indexing based single cell RNA seq of isolated nuclei (paraformaldehyde-fixed) from 61 snap-frozen C57BL/6J embryos collected at five daily intervals (Cao et al., 2019). Their capture methodology, which did not require physical isolation of cells, yielded barcoded libraries where each cell could be indexed by its originating embryo. Across 26,183 DEGs, they identified 2,863 cell-type-specific marker genes and this enabled annotation of 38 main cell clusters (Figure 4b).

The corresponding Mouse Organogenesis Cell Atlas (MOCA, (http://atlas.gs.washington.edu/mouse-rna/) sets the stage for conducting "virtual experiments" to gain deeper analysis of cell state landscapes. From the 38 main cell type clusters produced by t-SNE plots of mouse embryos collected E9.5–E13.5, the deeper analysis based on the various state trajectories produced 655 subclusters (Cao et al., 2019). For example, pseudo-temporal ordering of Apical Ectodermal Ridge (AER) cells based on 710 DEGs connected to the known markers for AER-specific expression discriminated a trajectory distinct from general epithelium, where this transitory cell type increased to peak frequency on E10.5–E11.5 (Cao et al., 2019). The cell state landscape in the mouse embryo, like zebrafish, did not strictly align with the cell lineage map.

5.2 | Cardiogenesis

Congenital heart defects (CHDs) can arise following disruption of cardiac progenitor cells or multipotent neural crest cells. In mouse, for example, *Hand2* genetic deficiency result in CHDs but linking pathogenesis to progenitor cell types that are affected by such mutations has

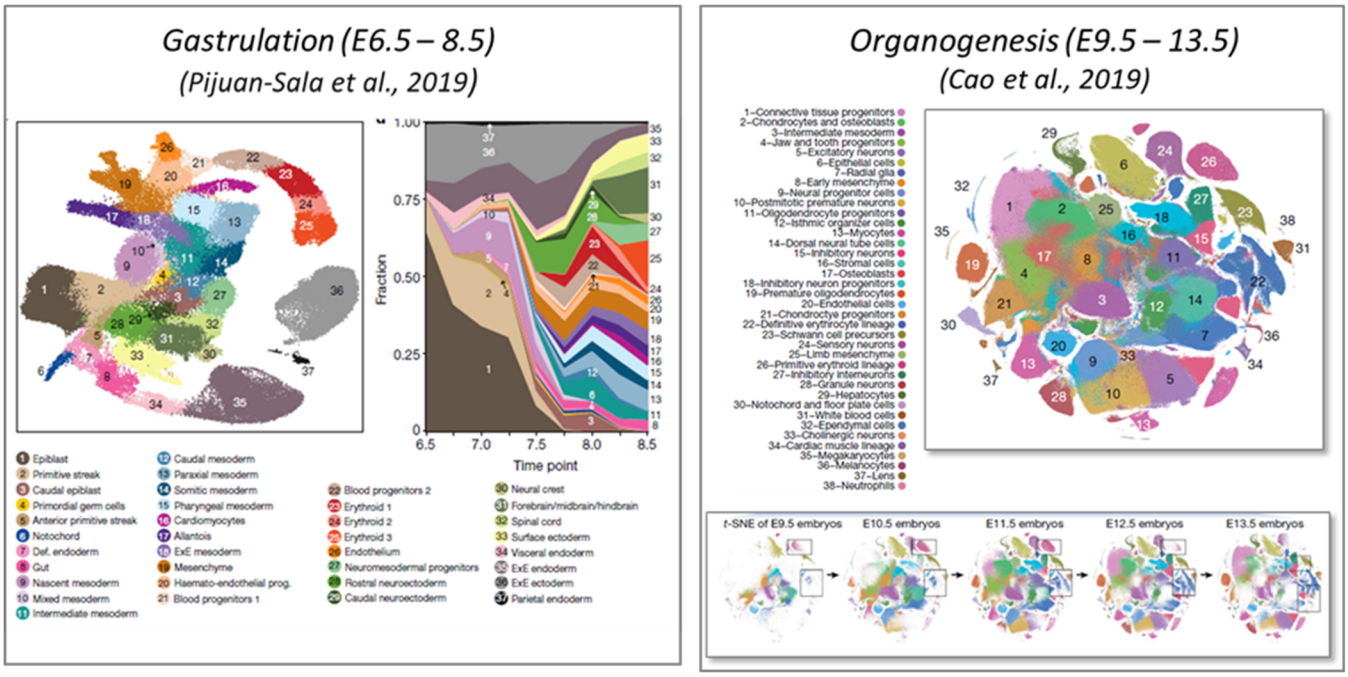

FIGURE 4 Profiling cell developmental trajectories in the mouse embryo using scRNA-seq. (Left) Gastrulation-early organogenesis when most cell lineages of the embryo proper emerge; t-SNE lineage identified 37 main clusters staged from 116,312 cells epiblast (E6.5) to headfold (E8.5), graphed in pseudotime by cell frequency (Pijuan-Sala et al., 2019). (Right) composite t-SNE annotated for 38 main cell clusters during organogenesis, the period when most organ systems form; pseudotime representation is superimposed on the composite t-SNE structure for the 151 K cells recorded on E9.5, 370 K cells on E10.5, 603 K cells on E11.5, 468 K cells on E12.5, and 435 K cells on E13.5 (Cao et al., 2019)

remained a challenge. Single-cell profiling captured 36,000 cells from the cardiogenic region of mouse embryos at three developmental landmarks: cardiac crescent (E7.75); heart tube (E8.25); and heart loop (E9.25) (de Soysa et al., 2019). Single cell transcriptomics identified *Hand2* as a critical lineage specifier of myocardial cells, consistent with defects of the outflow tract and severe hypoplasia of the right ventricle observed in *Hand2*-deficient mice (Figure 5). Unexpectedly, however, this dysregulation applied only to specification of myocardial progenitor cells destined for the cardiac outflow tract and not the right ventricle.

To better understand the discordance between single cell lineage analysis and observed phenotype (e.g., failure to link right ventricular hypoplasia to deficient *Hand2* expression in wild-type embryos), scRNA-seq analysis was performed on the secondary heart field from *Hand2*-null embryos. This confirmed transcriptional dysregulation with loss of *Hand2* function in the heart loop at E7.75, well prior to overt dysmorphogenesis, and furthermore revealed dysregulation of all-trans retinoic acid (ATRA) signaling as the primary basis of right ventricular hypoplasia. This was linked mechanistically to ATRA-induced posteriorization of the prospective right ventricle into a more anterior (atrial-like) fate (de Soysa et al., 2019). This is one of the few examples that shows a single cell data set of a frank birth defect and highlights the potential application of the approach.

5.3 | Pluripotency

Molecular profiling studies have shown that pluripotent mESCs most closely resemble the epiblast, which is the precursor of almost all cell lineages in the embryo (Cheng et al., 2019; Han, Chen, et al., 2018; Klein et al., 2015; Pijuan-Sala et al., 2019). Ahead of gastrulation, scRNA-seq was used to build a molecular roadmap that highlights epiblast cells transiting through pluripotency states as they acquire the propensity for primitive streak formation (Cheng et al., 2019). The epiblast responds to signals from extraembryonic tissues, gradually exits from the ground-state pluripotency, and is primed for multi-lineage specification. Mouse stem cell lines derived from the embryoblast (mESCs) and epiblast (EpiSCs) are functionally and morphologically distinct from one another and are *in vitro* counterparts in a distinct developmental progression from: (1) naïve pluripotency (ground-state) represented by

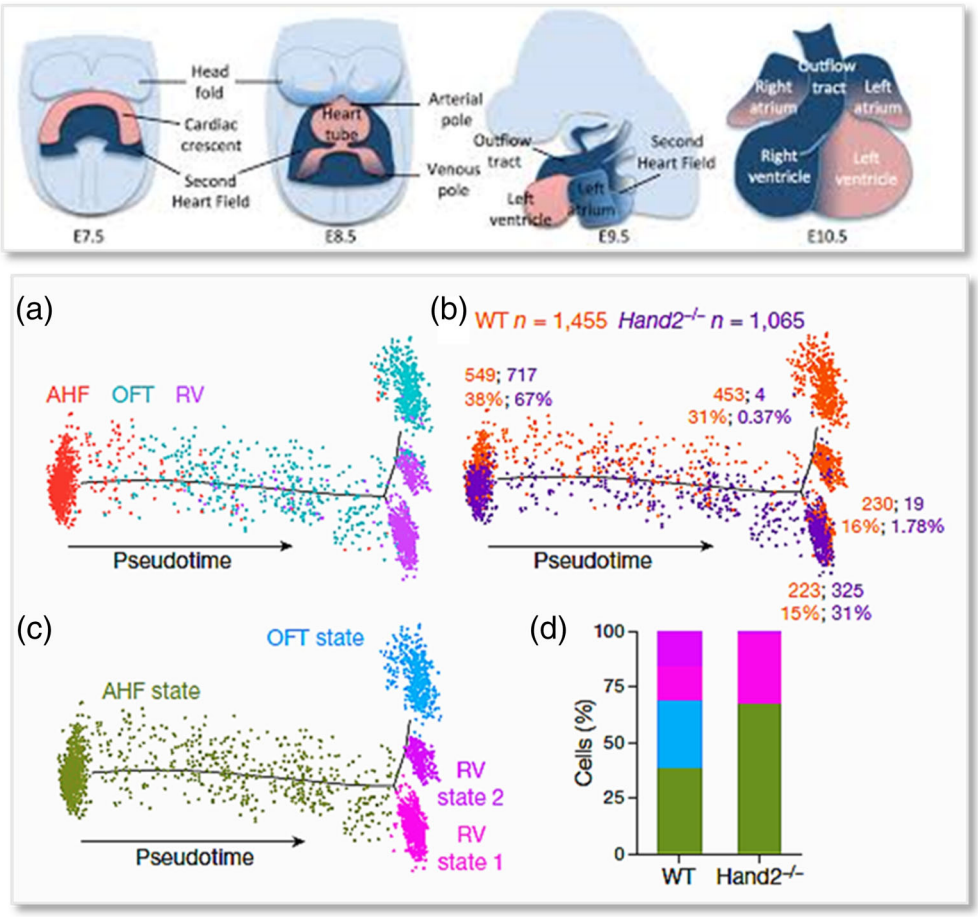

FIGURE 5 Profiling early cardiogenic trajectories in the mouse embryo. (Top) Stages of cardiogenesis depicted in the mouse embryo at the cardiac crescent (E7.5), heart loop (E8.5), and outflow tract/secondary heart field stage (E9.5) (from http://www.ibdm.univ-mrs.fr/equipw/genetic-control-of-heart-devlopment/) (Bottom) scRNA-seq profiling of the heart in pseudotime comparing cell cluster sizes in wild-type and Hand2-null embryos. Pseudotime trajectory for the anterior heart field (AHF), outflow tract (OFT), and right ventricle (RV) at E8.25 colored by cluster identity (a), genotype (b), and cell state (c) (de Soysa et al., 2019)

preimplantation inner cell mass and cultured mESCs; (2) intermediate epiblast-like cells (pregastrula); and (3) primed-pluripotency (mid-late gastrulation). Cheng et al. (2019) used scRNA-seq of 1,724 cells collected from 28 embryos at E5.25, E5.5, E6.25, and E6.5 (pre-streak) to track molecular states as the epiblast undergoes its putative pluripotency continuum. From 3,000 HVGs, t-SNE mapped three main cell clusters: epiblast (768 cells clustering in the *Pouf5f1* domain); visceral endoderm (671 cells clustering in the *Amn* domain), and extraembryonic ectoderm (ExE, 285 cells clustering in the *Bmp4* domain).

5.4 | mESCs

InDrop barcoding has been applied to mESCs as a model for assessing the challenges in parallel processing of thousands of cells and comprehensive mRNA capture (Klein et al., 2015). Here, they compared mESCs ± LIF (Leukemia inhibitory factor, a cytokine that maintains pluripotency) withdrawal for >10,000 barcoded cells and 3,034 randomly sampled mESCs differentiating over 7-days. For 935 mESCs, HVGs were enriched for transcriptional regulation and pluripotency, with most reflecting heterogeneity between ICM (high pluripotency) and epiblast (low pluripotency) states. Consistent with this, t-SNE plots showed a high- to low-pluripotency state continuum upon LIF withdrawal reflecting predominantly epiblast and primitive endoderm lineages thereby recapitulating the inner cell mass (embryoblast) *in vivo*. They found little evidence of patterning at 0-day, weak patterning at 2-day, strong patterning at 4-day, and resolving at 7-days. Therefore, mESCs are in a "ground-state" of naïve pluripotency that can be maintained with LIF. Soon after implantation (*in vivo*) or LIF withdrawal (*in vitro*), the ICM or mESC population, respectively, progresses into a "primed-state" of lineage specification characterized by promiscuous gene expression that becomes further refined as pluripotency is progressively lost during overt differentiation. While stem cell lines can be derived from the postimplantation EpiSCs, they are lineage-primed (e.g., low pluripotency). Human induced pluripotent stem cells (iPSCs) have the molecular and functional identity of post-implantation lineage primed EpiSCs.

5.5 | hESCs

Embryoid bodies (EB) derived from human embryonic stem cells (hESCs) *in vitro* recapitulate embryonic ectoderm and mesoendoderm. Single H9 hESCs ($n = 4,822$) were captured for scRNA profiling at a read depth of 5,000 genes per cell at naïve ($n = 1,491$), primed ($n = 695$), and EB ($n = 2,636$) stages (683 cells at Day 4, 1953 cells at Day 8) (Han, Chen, et al., 2018). They report four main clusters: two (naïve, primed) relatively homogeneous and two (EB-ectoderm and EB-mesendoderm) heterogeneous due to spontaneous differentiation. Based on DEGs, they mapped the cellular landscape for primed EB lineages showing weak heterogeneity on Day 4 versus Day 8 (as might be expected); in this case, however, they defined three progenitor lines on EB-4 (unspecified, neural, mesendodermal) and six progenitor lineages on EB-8 (muscle, stromal, endothelial, neural, epithelial, liver). Construction of an early differentiation trajectory of EB-8 in pseudotime revealed two main branches (neuroectoderm, mesoendoderm), similar to *in vivo* development of primed EPI into embryonic ectoderm + primitive streak (embryonic mesoderm and endoderm). These authors (Han, Chen, et al., 2018) also showed that the transitional states are interconvertible under certain conditions *in vitro*. For example, primed H9 hESCs can be stably reset to the naïve state 15–20 days in culture with commercial "RSeT" medium (Han, Chen, et al., 2018). This system provides a model to build "reset trajectories" in pseudotime during H9 culture Day 0 to Day 20.

6 | SEX DIFFERENTIATION

6.1 | Gonad specification

Recent studies have applied single-cell profiling to later developmental processes such as sex differentiation. Gonadal assembly from somatic cells in the male and female involves dimorphic cell lineage divergence from a sexually indifferent gonadal rudiment. This involves gonadal support cells (pre-Sertoli cells in the male, pregranulosa cells in the female) and steroidogenic cells (Leydig cells, Theca cells). To deconvolute lineage specification in the mouse embryo, scRNA-seq analysis was performed (Stevant et al., 2019). Commitment to the supporting cell lineage involves a common intermediate differentiation step before the emergence of pre-Sertoli or pre-granulosa cells. A non-sex-specific transcriptomic program was identified as these supporting cells acquire their identity. In chick embryos, scRNA-seq analysis showed that pre-Sertoli cells and pregranulosa cells were not derived from the coelomic epithelium but rather from a novel mesenchymal population (Estermann et al., 2020). These studies raise questions on the identity of the signals or factors that control the specification toward either the supporting or the steroidogenic fates during evolution and development.

6.2 | Germline differentiation

Single-cell RNA-seq analysis was performed on 2,167 germ cells and their gonadal niche cells from 29 female and male human embryos between 4 and 26 weeks of gestation (Li et al., 2017). t-SNE analysis clearly identified 17 clusters of which four clusters had germline-specific biomarkers for the female germline: mitotic phase, retinoic acid signaling-responsive phase, meiotic prophase, and oogenesis phase. They identified three clusters for the male germline: migrating phase, gonadal mitotic phase, and mitotic arrest phase. They observed reciprocal signaling interactions between germline cells and their respective gonadal niche cells, including activation of the bone morphogenic protein (BMP) and Notch signaling pathways. For example, male gonadal somatic cells specifically express Anti-Mullerian Hormone (AMH), and female gonadal somatic cells specifically express bone morphogenetic protein 2 (BMP2), whereas subpopulations of germline express the cognate receptor (BMPR1B).

7 | IMPLICATIONS FOR TERATOGENESIS

Although developmental toxicology has yet to experience scRNA-seq profiling in the next-generation blueprint for chemical testing (Thomas et al. 2019), these studies offer new insights into novel mechanisms as to how specific compounds might perturb early embryonic development. An example is shown for the effects of nicotine on gene expression dynamics in hESCs (Guo et al., 2019). Pregnant rodent studies have shown developmental toxicity with nicotine exposure. Guo et al. (2019) performed microdroplet RNA-seq on embryoid bodies from hESCs exposed to 10 μM nicotine (5,646 single cells) and control cultures (6,847 single cells). From ~3,000 median genes per cell, they identified six main progenitor cell lineages at Day 21 (muscle, hepatic, neural, stromal, epithelial, and endothelial). Interestingly, nicotine exposure increased genes for ligand-receptor pairs indicating the potential to increase cell-to-cell communication lines broadcast between specific cell types (Figure 6).

With recent breakthroughs in single cell technologies, a watershed of opportunity now exists to advance scientific understanding of functional cell states, paving the way to deeper knowledge of developmental processes and toxicities and opening new insights into when, where, and how developmental defects arise and the steps needed to reliably model human developmental toxicity (Scialli et al., 2018). One is to help map human developmental physiology from the molecular to the organism level at a level of detail fit for the purpose of toxicity testing. Cell atlases built with scRNA-seq and spatial mapping data are contributing to The Human Cell Atlas (HCA) project (www.humancellatlas.org) (Behjati, Lindsay, Teichmann, & Haniffa, 2018) that can be directly compared for a number of embryonic cell types catalogued with the Mouse Cell Atlas (MCA) (Han et al., 2018). The capacity to spatially dissect a target field by similarity in cell-level transcriptome response queried against MCA-HCA provides baseline information on gene expression dynamics as cells acquire specified fates during morphogenesis and differentiation and can facilitate the use of mouse models for human developmental defects.

Another opportunity from Scialli et al. (2018) is to integrate existing chemistry and toxicity knowledge (e.g., identify the major modes of action of human developmental toxicity, map the integrated Adverse Outcome Pathways (AOPs) for the purpose of toxicity testing, identify rate-limiting biological key events and related biomarkers, and design biomarker-related test systems). The use of scRNA-seq data in a dose response evaluation can provide important cell-level information concerning "sentinel cell" states that would predict toxicity prior to widespread organ or organism damage, where bulk averaging methodology would mask small, sentinel changes even in a seemingly homogeneous tissue or cell line. The power of scRNA-seq is to disentangle heterogeneous cell populations in close spatial proximity that have historically proven difficult to characterize transcriptionally using manual tissue dissection or reporter-gene based isolation.

Analyses of developmental trajectories reveal prospective cell types long before they become morphologically distinct. This can enhance building and testing of computational tools for toxicity prediction (integrate quantitative test output into an AOP network model, define thresholds of adversity at the integrated model level) (Scialli et al., 2018). Computational biology and simulation will inevitably play an essential role in translating cell-state dynamics into disease progression on a cell-by-cell and interaction-by-interaction basis. Computational algorithms for pseudo-temporal ordering of early development in SMOs and differentiating ESCs have started to define the developmental grammar through which pluripotent cells acquire their fates (e.g., programming, canalization; Cao et al., 2019; Wagner et al., 2018). Transitional cell states extracted from scRNA-seq data in pseudotime would essentially assign a time stamp to each cell in a heterogeneous population following a physiological stimulus or perturbation. Progression in a differentiation trajectory is asynchronous/discontinuous and can reveal critical bifurcation points foreshadowing developmental toxicity. For

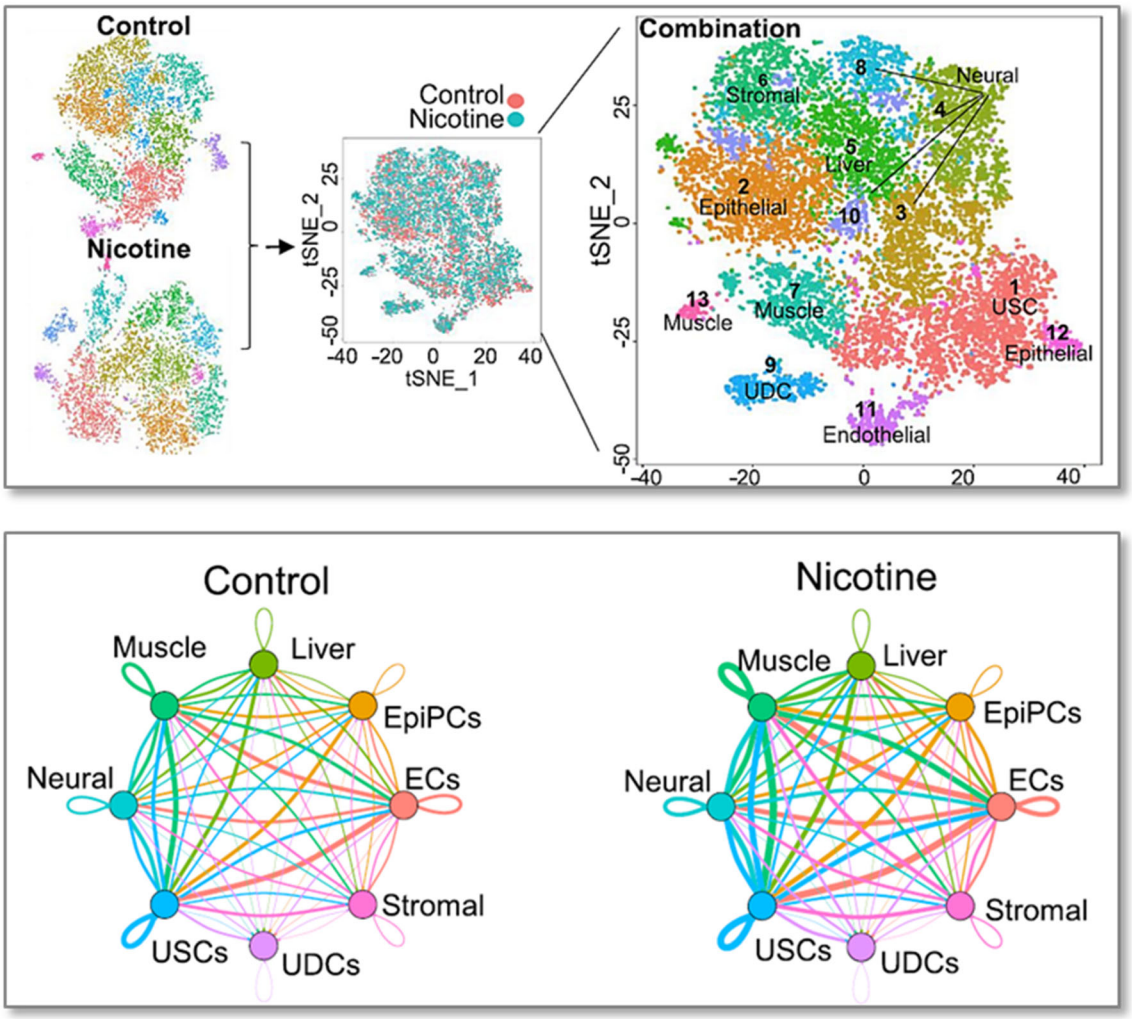

FIGURE 6 Profiling cell developmental trajectories in the ESCs using scRNA-seq. (Top) t-SNE plots from hESC-derived embryoid bodies on Day 21 of culture; control condition (n = 6,847 individual cells) and 10 μM nicotine. (Bottom) Nicotine exposure increased specific cell-to-cell communication pathways; directed acyclic graph connects ligands to receptors for target cell populations for ligand-receptor pairs (line thickness reflects ligand# in the coupled population) (Guo et al., 2019). See, for example, the thickness increase in pathways for ECs with muscle and USCs

developmental and reproductive toxicity, it has been a challenge to identify key events during normal development as well as to track impacted cells and processes along an altered developmental trajectory. Continuum gene expression manifolds reduce the dimensionality of cell–cell distances to virtual pseudotime state trajectories. This can embed toxicodynamic models within overall risk assessment paradigms.

8 | TRANSLATABILITY TO HUMAN RISK ASSESSMENT

Human health risk assessment is the process by which we collect scientific information on how chemicals, agents or events can impact human health. In risk assessment, there is the need for both exposure information and hazard information (toxicity). For developmental toxicity, this information is needed prior to conception, during gestation and postnatally throughout puberty in order to understand implications for children's health. Single cell transcriptomics offers a unique opportunity to understand impacts on specific target cells at different times in development. It provides a new way to track alterations in specific cells at specific locations and at specific stages of differentiation. And, it provides an unprecedented insider's view of cell behavior and contributions to organ and organism development. When temporal gene expression is linked with morphological location, these techniques will have tremendous power to answer questions about the sensitivity of specific cells to toxicant exposure in specific organs and in specific species, and their relevance to

prediction of human health effects. For example, are target cells present in only specific locations or are impacts only seen in specific species?

Although here in this review we focused on gastrulation-organogenesis, recent studies have applied single-cell profiling to later developmental processes such as lung maturation and brain development. For example, the airways of the lung are the primary sites of disease in asthma and cystic fibrosis. An scRNA-seq analysis of the cellular composition and hierarchy of the mouse tracheal epithelium and *in vivo* lineage tracing at 6–12 weeks of age identified a novel, specialized ionocyte as the major source of transcripts of the cystic fibrosis transmembrane conductance regulator in both mouse (*Cftr*) and human (*CFTR*) whereas previously it was thought that CFTR was expressed throughout the lung epithelium (Montoro et al., 2018; Plasschaert et al., 2018). As part of a forward strategy to resolve cell-type-specific spatial organization of the brain (Cembrowski, 2019), scRNA-seq has been used to characterize transcriptional dynamics in the neurogenic stem cell niche and cell-type-specific dysfunctions underlying impaired neurogenesis (Zywitza, Misios, Bunatyan, Willnow, & Rajewsky, 2018), reveal distinct transitional states during specification of neural and glial progenitors (Weng et al., 2019), assess transitional states in microglia activation during neuroinflammation (Sousa et al., 2018), and identify putative therapeutic targets for tumor progression in patient-specific cerebral organoid models (Krieger et al., 2020). These examples also show how single-cell profiling can allow improved comparisons of *in vitro* versus *in vivo* trajectories enhancing our knowledge of developmental timing and trajectories and thus informing experimental design and time of treatment for developmental toxicity testing.

A March 2019 workshop by the National Academy of Sciences recognized the unprecedented resolution and innovation of single cell profiling to examining biological systems and their perturbation by chemicals (Zhang et al., 2019). For precision toxicology, the concept of single-cell profiling has obvious appeal based on the sensitivity and specificity shown from its applications in developmental biology. However, for risk assessors interested in identifying levels of exposure for human populations without adverse effects, the detail in the scRNA may be overwhelming. Integration of scRNA-seq data into AOP-based frameworks can be useful to identify specific target cells and stages.

In conclusion, technological advances have now set the stage for single-cell profiling in the field of birth defects research and prevention for: (1) defining trajectories of developmental processes driving differentiation and function; (2) characterizing similarities/dissimilarities in cell types and functional states across species, tissues, and organs; (3) providing important information for establishing and testing data for relevant AOP frameworks; (4) qualifying *in vitro* data and *in silico* models for new approach methodologies that aim for less reliance on animal testing; and (5) improving our ability to identify early events and track disease trajectories with greater relevance to human development. Of course, some of the current limitations of single cell profiling technologies, such as very high costs, the sparsity of the data, the challenging computational analysis, and scalability point to the continued needs for technology development so that many experiments can be run in parallel. Like any rapidly evolving method, scRNA-seq faces challenges for science and technology development and with regards to knowing which application to use for these purposes and relevant quality control measures for transparency and reproducibility. An explosion of different processing and analytical methods have emerged in recent years and we anticipate improved understanding of which approaches might be better fit for one purpose or another in unraveling complex cell state trajectories during developmental processes and toxicities.

ACKNOWLEDGEMENTS

The authors wish to acknowledge Science Committee of the Society for Birth Defects Research and Prevention who organized this session, and especially Becca Isakower, Senior Program Manager of Society for Birth Defects Research and Prevention (formerly Teratology Society) for her gracious logistical support. We also thank Brian Chorley and Logan Everett at the USEPA's Center for Computational Toxicology and Exposure for their helpful comments on the manuscript.

CONFLICT OF INTEREST

The authors have no conflicts of interest to disclose.

DATA AVAILABILITY STATEMENT

Data sharing is not applicable to this article as no new data were created or analyzed in this study.

ORCID

Thomas B. Knudsen https://orcid.org/0000-0002-5036-596X

REFERENCES

Becht, E., McInnes, L., Healy, J., Dutertre, C.-A., Kwok, I. W. H., Ng, L. G., ... Newell, E. W. (2019). Dimensionality reduction for visualizing single-cell data using UMAP. *Nature Biotechnology*, *37*, 38–44.

Behjati, S., Lindsay, S., Teichmann, S. A., & Haniffa, M. (2018). Mapping human development at single-cell resolution. *Development*, *145*, dev152561. https://doi.org/10.1242/dev.152561

Briggs, J. A., Weinrab, C., Wagner, D. E., Megason, S., Peshkin, L., Kirschner, M. W., & Klein, A. M. (2018). The dynamics of gene expression in vertebrate embryogenesis at single-cell resolution. *Science*, *360*, eaar5780. https://doi.org/10.1126/science.aar5780

Cao, J., Packer, J. S., Ramani, V., Cusanovich, D. A., Huynh, C., Daza, R., ... Shendure, J. (2017). Comprehensive single-cell transcriptional profiling of a multicellular organism. *Science*, *357*, 661–667.

Cao, J., Spielmann, M., Qiu, X., Huang, X., Ibrahim, D. M., Hill, A. J., ... Shendure, J. (2019). The single-cell transcriptional landscape of mammalian organogenesis. *Nature*, *566*, 496–502. https://doi.org/10.1038/s41586-019-0969-x

Cembrowski, M. S. (2019). Single-cell transcriptomics as a framework and roadmap for understanding the brain. *Journal of Neuroscience Methods*, *326*(10835), 108353.

Chan, M. M., Smith, Z. D., Grosswendt, S., Kretzmer, H., Norman, T. M., Adamson, B., ... Weissman, J. S. (2019). Molecular recording of mammalian embryogenesis. *Nature*, *570*, 77–82.

Cheng, S., Pei, Y., He, L., Peng, G., Reinius, B., Tam, P. P. L., ... Deng, Q. (2019). Single-cell RNA-seq reveals cellular heterogeneity of pluripotency transition and X chromosome dynamics during early mouse development. *Cell Reports*, *26*, 2593–2607.

de Soysa, T. Y., Ranade, S. S., Okawa, S., Ravichandran, S., Huang, Y., Salunga, H. T., ... Srivastava, D. (2019). Single-cell analysis of cardiogenesis reveals basis for organ-level developmental defects. *Nature*, *572*, 120–124.

Estermann, M. A., Williams, S., Hirst, C. E., Powell, D., Major, A. T., & Smith, C. A. (2020). Insights into gonadal sex differentiation provided by single-cell transcriptomics in the chicken embryo. *Cell Reports*, *31*, 107491.

Farrell, J. A., Wang, Y., Riesenfeld, S. J., Shekhar, K., Regev, A., & Schier, A. F. (2018). Single-cell reconstruction of developmental trajectories during zebrafish embryogenesis. *Science*, *360*, eaar3131. https://doi.org/10.1126/science.aar3131

Guo, H., Tian, L., Zhang, J. Z., Kitani, T., Paik, D. T., Lee, W. H., & Wu, J. C. (2019). Single-cell RNA sequencing of human embryonic stem cell differentiation delineates adverse effects of nicotine on embryonic development. *Stem Cell Reports*, *12*, 772–786.

Hallgrímsson, B., Willmore, K., & Hall, B. K. (2002). Canalization, developmental stability, and morphological integration in primate limbs. *Yearbook of Physical Anthropology*, *45*, 131–158.

Han, X., Chen, H., Huang, D., Chen, H., Fei, L., Cheng, C., ... Guo, G. (2018). Mapping human pluripotent stem cell differentiation pathways using high throughput single-cell RNA-sequencing. *Genome Biology*, *19*, 47. https://doi.org/10.1186/s13059-018-1426-0

Han, X., Wang, R., Zhou, Y., Fei, L., Sun, H., Lai, S., ... Guo, G. (2018). Mapping the mouse cell atlas by microwell-seq. *Cell*, *172*, 1091–1107.

Karaiskos, N., Wahle, P., Alles, J., Boltengagen, A., Ayoub, S., Kipar, C., ... Zinzen, R. P. (2017). The Drosophila embryo at single-cell transcriptome resolution. *Science*, *358*, 194–199.

Keller, P. J., Schmidt, A. D., Wittbrodt, J., & Stelzer, E. H. K. (2008). Reconstruction of zebrafish early embryonic development by scanned light sheet microscopy. *Science*, *322*, 1065–1069.

Kiselev, V. Y., Andrews, T. S., & Hemberg, M. (2019). Challenges in unsupervised clustering of single-cell RNA-seq data. *Nature Reviews Genetics*, *20*, 273–282.

Klein, A. M., Mazutis, L., Akartuna, I., Tallapragada, N., Veres, A., Li, V., ... Kirschner, M. W. (2015). Droplet barcoding for single-cell transcriptomics applied to embryonic stem cells. *Cell*, *161*, 1187–1201.

Krieger, T. G., Tirier, S. M., Park, J., Jechow, K., Eisemann, T., Peterziel, H., ... Conrad, C. (2020). Modeling glioblastoma invasion using human brain organoids and single-cell transcriptomics. *Neuro-Oncology*, *22*, 1138–1149. https://doi.org/10.1093/neuonc/noaa091

Leuken, M. D., & Theis, F. J. (2019). Current best practices in single-cell RNA-seq analysis: A tutorial. *Molecular Systems Biology*, *15*, e8746.

Li, L., Dong, J., Yan, L., Yong, J., Liu, X., Hu, Y., ... Qiao, J. (2017). Single-cell RNA-seq analysis maps development of human germline cells and gonadal niche interactions. *Cell Stem Cell*, *20*, 858–873.

McDole, K., Guignard, L., Amat, F., Berger, A., Malandain, G., Royer, L. A., ... Keller, P. J. (2018). In toto imaging and reconstruction of postimplantation mouse development at the single cell level. *Cell*, *175*, 859–876.

McKenna, A., & Gagnon, J. A. (2019). Recording development with single cell dynamic lineage tracing. *Development*, *146*, dev169730. https://doi.org/10.1242/dev.169730 (10 pages).

Megason, S. G. (2009). In toto imaging of embryogenesis with confocal time-lapse microscopy. *Methods in Molecular Biology*, *546*, 317–332.

Montoro, D. T., Haber, A. L., Biton, M., Vinarsky, V., Lin, B., Birket, S. E., ... Rajagopal, J. (2018). A revised airway epithelial hierarchy includes CFTR-expressing ionocytes. *Nature*, *560*, 319–324.

Pijuan-Sala, B., Griffiths, J. A., Guibentif, C., Hiscock, T. W., Jawaid, W., Calero-Nieto, F. J., ... Göttgens, B. (2019). A single-cell molecular map of mouse gastrulation and early organogenesis. *Nature*, *566*, 490–495. https://doi.org/10.1038/s41586-019-0933-9

Plass, M., Solana, J., Wolf, F. A., Ayoub, S., Misios, A., Glažar, P., ... Rajewsky, N. (2018). Cell type atlas and lineage tree of a whole complex animal by single-cell transcriptomics. *Science*, *360*, eaaq1723 (10 pages).

Plasschaert, L. W., Žilionis, R., Choo-Wing, R., Savova, V., Knehr, J., Roma, G., ... Jaffe, A. B. (2018). A single-cell atlas of the airway epithelium reveals the CFTR-rich pulmonary ionocyte. *Nature*, *560*, 377–381.

Saelens, W., Cannoodt, R., Todorov, H., & Saeys, Y. (2019). A comparison of single-cell trajectory inference methods. *Nature Biotechnology*, *37*, 547–554.

Scialli, A. R., Daston, G. P., Chen, C., Coder, P. S., Euling, S. Y., Foreman, J., ... Thompson, K. E. (2018). Rethinking developmental toxicity testing: Evolution or revolution? *Birth Defects Research*, *110*, 840–850.

Sladitschek, H. L., Fiuza, U.-M., Pavlinic, D., Benes, V., Hufnagel, L., & Neveu, P. A. (2020). MorphoSeq: Full single-cell transcriptome dynamics up to gastrulation in a chordate. *Cell*, *181*, 922–935.

Sousa, C., Golebiewska, A., Poovathingal, S. K., Kaoma, T., Pires-Afonso, Y., Martina, S., ... Michelucci, A. (2018). Single-cell transcriptomics reveals distinct inflammation induced microglia signatures. *EMBO Reports*, *19*, e46171.

Stevant, I., Kuhne, F., Greenfield, A., Chaboissier, M.-C., Dermitzakis, E. T., & Nef, S. (2019). Dissecting cell lineage specification and sex fate determination in gonadal somatic cells using single-cell transcriptomics. *Cell Reports*, *26*, 3272–3283.

Thomas, R. S., Bahadori, T., Buckley, T. J., Cowden, J., Deisenroth, C., Dionisio, K. L., … Williams, A. J. (2019). The next generation blueprint of computational toxicology at the U.S. environmental protection agency. *Toxicological Sciences*, *169*, 317–332. http://dx.doi.org/10.1093/toxsci/kfz058.

Wagner, D. E., Weinreb, C., Collins, A. M., Briggs, J. A., Megason, S. G., & Klein, A. M. (2018). Single-cell mapping of gene expression landscapes and lineage in the zebrafish embryo. *Science*, *360*, 981–987.

Weng, Q., Wang, J., Wang, J., He, D., Cheng, Z., Zhang, F., … Lu, Q. R. (2019). Single-cell transcriptomics uncovers glial progenitor diversity and cell fate determinants during development and gliomagenesis. *Cell Stem Cell*, *24*, 707–723.

Wong, M. D., van Eede, M. C., Spring, S., Jevtic, S., Boughner, J. C., Lerch, J. P., & Henkelman, R. M. (2019). 4D atlas of the mouse embryo for precise morphological staging. *Development*, *142*, 3583–3591.

Zhang, Q., Caudle, W. M., Pi, J., Bhattacharya, S., Andersen, M. E., Kaminski, N. E., & Conolly, R. B. (2019). Embracing systems toxicology at single-cell resolution. *Current Opinion in Toxicology*, *16*, 49–57.

Ziegenhaein, C., Vieth, B., Parekh, S., Reinius, B., Guillaumet-Adkins, A., Smets, M., … Enard, W. (2017). Comparative analysis of single-cell RNA sequencing methods. *Molecular Cell*, *65*, 631–643.

Zywitza, V., Misios, A., Bunatyan, L., Willnow, T. E., & Rajewsky, N. (2018). Single-cell transcriptomics characterizes cell types in the subventricular zone and uncovers molecular defects impairing adult neurogenesis. *Cell Reports*, *25*, 2457–2469.

How to cite this article: Knudsen TB, Spielmann M, Megason SG, Faustman EM. Single-cell profiling for advancing birth defects research and prevention. *Birth Defects Research*. 2021;113: 546–559. https://doi.org/10.1002/bdr2.1870